

## Article

# Microstructure and Mechanical Properties of GH4169 Superalloy and Si<sub>3</sub>N<sub>4</sub> Ceramic Joints Brazed with AgCuTi/Cu foam/AgCuTi Compositing Filler

Xiaohong Yang<sup>1</sup>, Yang Xue<sup>2,\*</sup> , Shenggang Wang<sup>1</sup>, Jianya Ge<sup>1</sup>, Yuan Chen<sup>1</sup>, Zhengzhong Zhang<sup>1</sup>, Jinhua Tang<sup>1</sup> and Junjian Xiao<sup>3,\*</sup>

<sup>1</sup> Academician Expert Workstation, Jinhua Polytechnic, Jinhua 321017, China

<sup>2</sup> School of Materials Science Engineering, Anhui Polytechnic University, Wuhu 241000, China

<sup>3</sup> College of Mechanical Engineering, Quzhou University, Quzhou 324000, China

\* Correspondence: xueyang6357@163.com (Y.X.); xjj919@sohu.com (J.X.); Tel.: +86-191-5562-8726 (Y.X.)

**Abstract:** GH4169 superalloy and Si<sub>3</sub>N<sub>4</sub> ceramics were vacuum-brazed with AgCuTi+Cu foam composite filler. The effect of brazing temperature on the microstructure and mechanical properties of the GH4169/Si<sub>3</sub>N<sub>4</sub> joint was studied. The results show that the interface microstructure of the GH4169/Si<sub>3</sub>N<sub>4</sub> joint is the GH4169 superalloy/TiCu+Ti<sub>2</sub>Ni+TiCu<sub>2</sub>+Ag(s, s)+TiCu<sub>4</sub>+Cu(s, s)+TiN+Ti<sub>5</sub>Si<sub>3</sub>/Si<sub>3</sub>N<sub>4</sub> ceramics. With the increase in brazing temperature, the element diffusion between the base metal and the brazing filler intensifies, and the interfacial reaction layer thickens, which is conducive to the improvement of shear strength. At 850 °C, the maximum shear strength of the joint is 196.85 MPa. After further increases in the brazing temperature, Cu foam dissolves completely, and the Ti-Cu intermetallic compounds increase, which is harmful to the shear strength due to the increases in the brittle phase. However, when the brazing temperature reaches 910 °C, the shear strength of the brazing joint slightly increases under the combined effect of the Ti-Cu intermetallic compounds and the thickness of the reaction layer.

**Keywords:** GH4169; Si<sub>3</sub>N<sub>4</sub>; Cu foam; microstructures; mechanical properties; brazing



**Citation:** Yang, X.; Xue, Y.; Wang, S.; Ge, J.; Chen, Y.; Zhang, Z.; Tang, J.; Xiao, J. Microstructure and Mechanical Properties of GH4169 Superalloy and Si<sub>3</sub>N<sub>4</sub> Ceramic Joints Brazed with AgCuTi/Cu foam/AgCuTi Compositing Filler.

*Coatings* **2022**, *12*, 1496.  
<https://doi.org/10.3390/coatings12101496>

Academic Editor: Maria Bignozzi

Received: 4 September 2022

Accepted: 5 October 2022

Published: 7 October 2022

**Publisher's Note:** MDPI stays neutral with regard to jurisdictional claims in published maps and institutional affiliations.



**Copyright:** © 2022 by the authors. Licensee MDPI, Basel, Switzerland. This article is an open access article distributed under the terms and conditions of the Creative Commons Attribution (CC BY) license (<https://creativecommons.org/licenses/by/4.0/>).

## 1. Introduction

Si<sub>3</sub>N<sub>4</sub> ceramics have the unique advantages of high strength, high hardness, corrosion resistance, oxidation resistance, and wear resistance [1]. It has been used in wide engineering applications, such as missile radome, satellite antenna, and aerospace [2,3]. However, the inherent brittleness and poor machinability of Si<sub>3</sub>N<sub>4</sub> ceramics limit its application [4–6]. Joining Si<sub>3</sub>N<sub>4</sub> ceramics with metal materials to form composites is an effective method to manufacture complicated component [7,8]. The ceramic-metal combination will take full advantage of the respective strengths of these two materials and has been used in rocker arm, ceramic turbocharger rotors, and vacuum electrodes [9–11]. At present, many studies have been conducted to join Si<sub>3</sub>N<sub>4</sub> ceramics with metals. Zhao et al. [12] successfully brazed Si<sub>3</sub>N<sub>4</sub> ceramic and Ti46Al2Cr2Nb alloy with AgCu powder filler. It was found that the surface metallization of Si<sub>3</sub>N<sub>4</sub> ceramic through the laser induction process can promote the effective filling of filler alloy in the brazing seam. Guo et al. [13] successfully brazed Si<sub>3</sub>N<sub>4</sub> ceramics and invar alloy with AgCuTi active filler, and the shear strength of the joint can be further improved by added nickel foam in the filler metal. So far, brazing has been considered by researchers as one of the most suitable technologies for joining ceramic-ceramic or ceramic-metal joints [14]. Due to the excellent high temperature properties of GH4169 superalloy, it has been widely used in industrial gas turbines and aero-engine components. However, the GH4169 superalloy is difficult to meet the special requirement of new high temperature components. Therefore, joining GH4169 superalloy to Si<sub>3</sub>N<sub>4</sub> ceramics showed great application value in high-temperature component areas.

In the current research, brazing was introduced to join  $\text{Si}_3\text{N}_4$  ceramics and GH4169 superalloy. GH4169 superalloy has attracted extensive attention due to the high-temperature strength, and good oxidation resistance. It is considered as an ideal material for making turbine blades and discs [15–17]. The obtained  $\text{Si}_3\text{N}_4$  ceramic/GH4169 superalloy joint is expected to be used in the aerospace field [18].

Due to the coefficient of thermal expansion (CTE) mismatch between  $\text{Si}_3\text{N}_4$  ceramics and GH4169 superalloys, the residual stresses are unavoidable. It can deteriorate mechanical properties of the joints greatly [19]. Different kinds of methods such as the addition of active metal powder, use of pure metal interlayer or metal foam interlayer have been widely used to alleviate the residual stresses [20,21]. Previous studies showed that the active metal powder is hardly to disperse uniformly, and the addition of pure metal interlayer reduced the plasticity of the joints. Therefore, as a traditional interlayer, Cu foam was selected to braze  $\text{Si}_3\text{N}_4$  ceramics and GH4169 superalloy.

In this work, the AgCuTi filler with Cu foam added as the interlayer was used to vacuum braze Nickel-base superalloy (GH4169)/ $\text{Si}_3\text{N}_4$  ceramics at different brazing temperatures. The effects of brazing temperature on the microstructure and mechanical properties of the joint interface were studied. The purpose of the current research is to obtain a solid  $\text{Si}_3\text{N}_4$ /GH4169 joint and clarify the mechanism of brazing temperature on the microstructure and mechanical properties of the joint. The research will help to broaden the application field of  $\text{Si}_3\text{N}_4$  ceramic and GH4169 superalloy combinations.

## 2. Materials and Methods

The commercial  $\text{Si}_3\text{N}_4$  ceramic used in the experiment was purchased from Suzhou Kaifate Pottery Technology Co., Ltd., which was prepared by hot pressing sintering. The commercial GH4169 superalloy was purchased from Western Superconducting Materials Technology Co., Ltd. (the composition is shown in Table 1), the GH4169 superalloy and  $\text{Si}_3\text{N}_4$  ceramic were cut into 10 mm × 10 mm × 4 mm and 4 mm × 4 mm × 4 mm blocks for microstructure. Figure 1 shows the microstructure of the GH4169 superalloy, which is mainly composed of  $\gamma$  and  $\delta$  phase,  $\gamma$  phase is the matrix and  $\delta$  phase is the precipitated phase at the grain boundary. Two layers of AgCuTi with Cu foam additions were used to braze the GH4169 superalloy and  $\text{Si}_3\text{N}_4$  ceramic; the microstructure of Cu foam with a porosity rate of 80% was shown in Figure 2.

**Table 1.** Chemical composition of the GH4169 alloy.

Ni	Cr	Nb	Mo	Ti	Al	Si	Fe
53.88	17.90	5.50	3.10	1.04	0.52	0.06	18.00

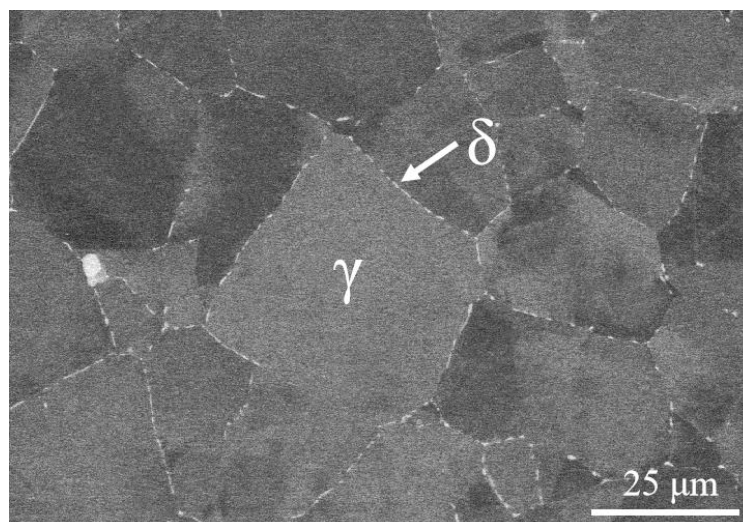


**Figure 1.** Microstructure of GH4169 superalloy.

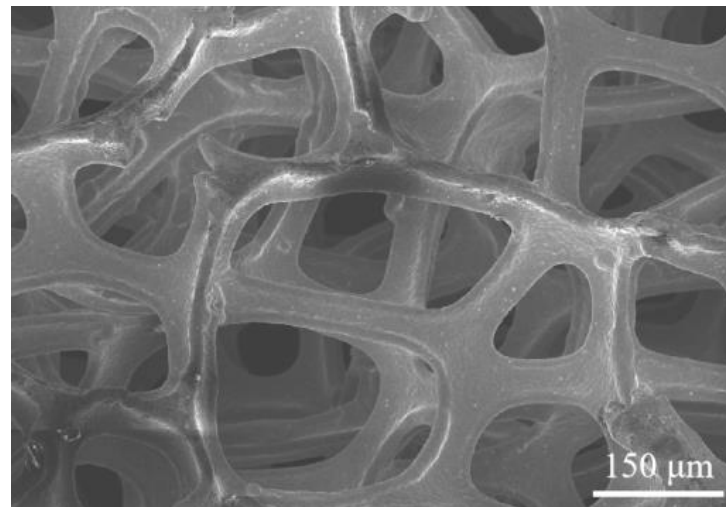


**Figure 2.** Microstructure of Cu foam.

The AgCuTi composite filler was prepared by a mixture of Ag-28Cu and Ti powder with the mass ratio of 95.5% to 4.5%; the composite filler was ground at a speed of 100 r/min for 8 h.

Before brazing, the brazing surface of GH4169 superalloy and Si<sub>3</sub>N<sub>4</sub> ceramic were ground to 2000 grit by SiC sandpapers. The AgCuTi composite filler compound and brazing flux were evenly mixed in a 9:1 ratio to make the solder paste, and the solder paste was applied to the surface to be brazed on the GH4169 superalloy, Si<sub>3</sub>N<sub>4</sub> ceramic, and Cu foam.

The sample was stacked into a component (as shown in Figure 3a) in the manner of Si<sub>3</sub>N<sub>4</sub> ceramic/AgCuTi filler/Cu foam/AgCuTi filler/GH4169 superalloy. The whole brazing process is less than  $8 \times 10^{-3}$  Pa vacuum brazing furnace. The samples were first heated to 400 °C at a rate of 5 °C/min, holding for 30 min, to ensure the evaporation of the brazing paste and the uniform the temperature, and then heated at a rate of 5 °C/min to the target brazing temperature (820 °C, 850 °C, 880 °C, 910 °C) for 15 min, and 5 samples were brazed at different brazing temperatures. Subsequently, the samples were cooled to room temperature at 5 °C/min. The thermal cycling curve of the brazing process is shown in Figure 4.

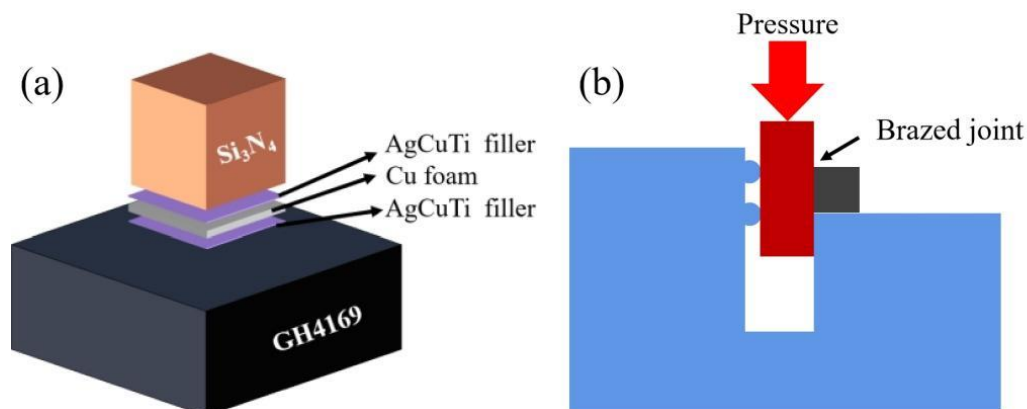


**Figure 3.** (a) Schematic diagram of sample assembly; (b) shear test.

Scanning electron microscopy (SEM) (Hitachi, Tokyo, Japan) and Energy dispersive spectrometer (EDS) (Ametek, Berwyn, IL, USA) were used to analyze the microstructure of the GH4169/Si<sub>3</sub>N<sub>4</sub> brazing joints. Phase identification was carried out by X-ray diffraction (XRD) (Bruker, Billerica, Germany). The shear test of the joint was carried out at a constant rate of 0.6 mm/min at room temperature and 50% humidity by MTS series 370 electronic universal testing machine (MTS, Eden Prairie, MN, USA) as shown in Figure 3b. After the shear test, the fracture morphology and fracture path were analyzed by SEM.

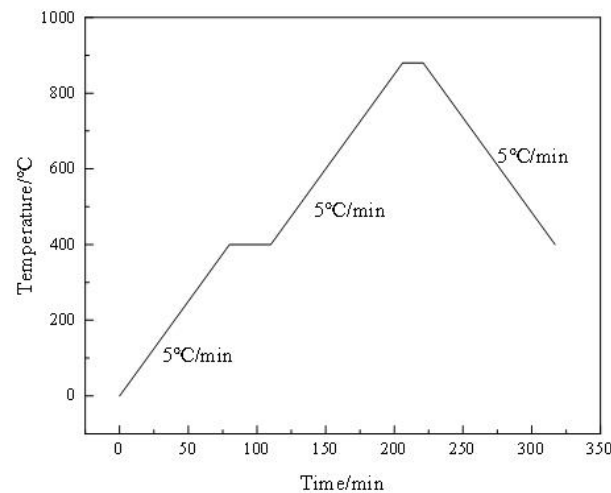


**Figure 4.** Thermal cycling curve of brazing.

### 3. Results and Discussion

#### 3.1. Microstructure of the GH4169/Si<sub>3</sub>N<sub>4</sub> Joints

Figure 5 shows the interfacial microstructure of GH4169/Si<sub>3</sub>N<sub>4</sub> joints brazed by AgCuTi filler with or without Cu foam addition at 850 °C for 15 min. As shown in Figure 5a and no defects can be found in the joints, which shows good bonding between the GH4169 superalloy and Si<sub>3</sub>N<sub>4</sub> ceramic. The brazing joint can be divided into three zones. Zones I and III are the reaction layer at the substrate side, respectively. As shown in Figure 5c,d, higher magnification of zones I and III shows that the reaction layer mainly composed of the phases, marked as A, B, C, D, E, F and G phase. For comparison, Figure 5b shows the microstructure of GH4169/Si<sub>3</sub>N<sub>4</sub> joint without Cu foam addition. It can also be seen that, without Cu foam addition, the brazing seam can also be divided into three zones, which are marked as zone 1, 2 and 3. With the addition of Cu foam, the volume fraction of white phase decreases and the gray phase increases greatly. The detailed phase constitution in the brazing joints was detected by XRD, and the results are shown in Figure 6. It can be seen that with Cu foam addition, the brazing seam is mainly composed of TiCu, Ti<sub>2</sub>Ni, TiCu<sub>2</sub>, Ag (s,s), Cu (s,s), TiCu<sub>4</sub>, Ti<sub>5</sub>Si<sub>3</sub>+TiN.

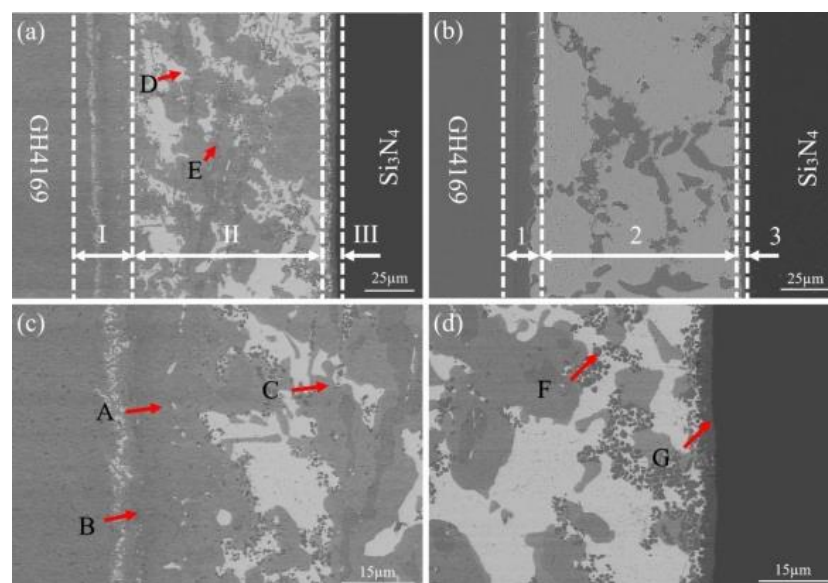


**Figure 5.** Microstructure of the GH4169/Si<sub>3</sub>N<sub>4</sub> joint brazed at 850 °C for 15 min: (a) the joint brazed with Cu foam; (b) the joint brazed without Cu foam; (c) high magnification image of the zone I; (d) high magnification image of the zone III.

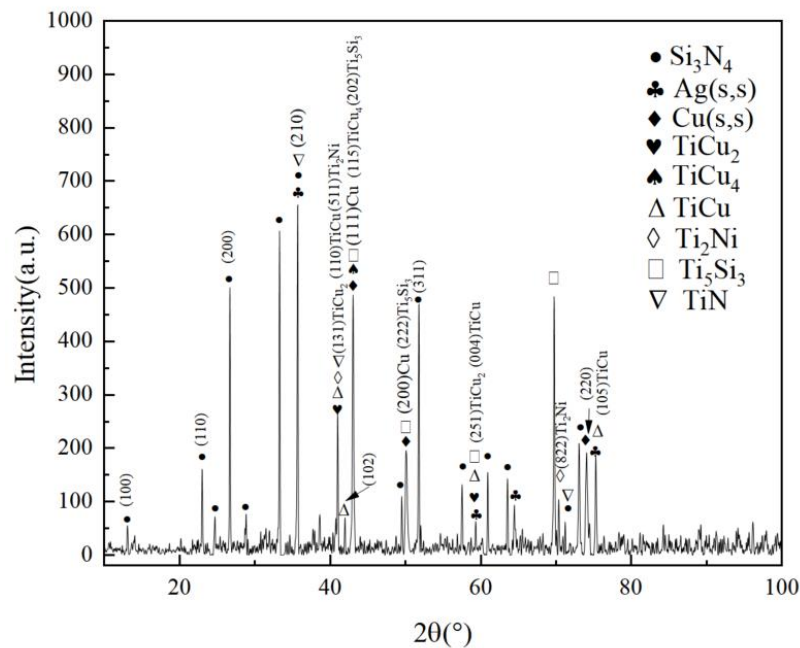


Figure 6. XRD patterns of the GH4169/AgCuTi+Cu foam/Si<sub>3</sub>N<sub>4</sub> joint brazed at 850 °C.

In order to further determine the phases in the brazing seam, EDS was conducted. The chemical composition of each phase is listed in Table 2. It can be seen that phase A comprised 6.32% Ag, 64.04% Cu and 29.64% Ti (at.). The atomic ratio of Ti to Cu is about 1:2. Combined with XRD, it can be inferred as TiCu<sub>2</sub> phase [22,23]. Phase B contained 24.13% Ni, 5.54% Cr, 7.51% Fe, 1.09% Ag, 10.78% Cu and 50.95% Ti. The ratio of Ti to Ni is about 2:1, which would be regarded as Ti<sub>2</sub>Ni phase [24,25]. Phase C incorporating 95.74% Cu, which is determined to be Cu(s, s). Phase D is Ag(s, s) phase. The atomic proportion of Ti:Cu in phase E is 1:4, which is suggested to be the TiCu<sub>4</sub> phase [26,27]. Figure 5d shows the magnified microstructure of the Si<sub>3</sub>N<sub>4</sub> ceramic side. The reaction layer is composed of Ti, N and Si. It was inferred that the reaction layer is composed of the TiN and Ti<sub>5</sub>Si<sub>3</sub> by EDS and XRD analysis, which is consistent with the results of Si<sub>3</sub>N<sub>4</sub>/Ti6Al4V joints brazed with nano-Si<sub>3</sub>N<sub>4</sub> reinforced AgCuTi filler conducted by Zhao et al. [23]. During brazing, the molten AgCuTi composite filler released large amount of Ti, and Ti would diffuse to the Si<sub>3</sub>N<sub>4</sub> ceramic side and then reacted with Si<sub>3</sub>N<sub>4</sub> ceramics to form TiN and Ti<sub>5</sub>Si<sub>3</sub> phase [28,29]. Therefore, the interface microstructure of the GH4169/Si<sub>3</sub>N<sub>4</sub> joint brazed at 850 °C for 15 min is GH4169 superalloy/TiCu+Ti<sub>2</sub>Ni+TiCu<sub>2</sub>+Ag(s, s)+TiCu<sub>4</sub>+Cu(s, s)+TiN+Ti<sub>5</sub>Si<sub>3</sub>/Si<sub>3</sub>N<sub>4</sub> ceramic.

Table 2. EDS results for the chemical composition of the different phases in Figure 4 (at. %).

Position	Ni	Cr	Fe	Ag	Cu	Ti	Si	n	Possible Phases
A	-	-	-	6.32	64.04	29.64	-	-	TiCu <sub>2</sub>
B	24.13	5.54	7.51	1.09	10.78	50.95	-	-	Ti <sub>2</sub> Ni
C	-	-	-	1.49	95.74	1.76	0.95	0.06	Cu (s,s)
D	0.94	1.07	0.71	88.99	7.59	0.70	-	-	Ag (s,s)
E	-	-	-	1.32	78.42	20.26	-	-	TiCu <sub>4</sub>
F	4.01	5.98	6.02	3.54	37.10	43.55	-	-	TiCu
G	-	-	-	8.26	2.87	52.98	25.77	10.11	Ti <sub>5</sub> Si <sub>3</sub> +TiN

The element distribution of GH4169/Si<sub>3</sub>N<sub>4</sub> joints brazed with AgCuTi+Cu foam were characterized by map scanning, as shown in Figure 7. It can be seen that no cracks or pores can be found in the brazing joints. It reveals that affirmative interfacial bonding was achieved between the substrates and brazing filler. In this figure, Ag, Cu and Ti were the major elements distributed in the joints. Ag is mainly distributed among the light grey regions, whereas Cu and Ti are distributed in the dark grey regions, as shown in Figure 7d,e,i. The dissolution of Cu foam leads to the enrichment of Cu content in the brazing seam. Similar phenomena were also found by Zhang et al. [26]. At the GH4169 superalloy side, the reaction layer was formed by a high concentration of Cu and a small quantity of Ti addition, Ti was also enriched at the Si<sub>3</sub>N<sub>4</sub> side, which can react with Si<sub>3</sub>N<sub>4</sub> to form a thin layer of TiN and Ti<sub>5</sub>Si<sub>3</sub>, as shown in Figure 7e. Xin et al. [28] also found TiN and Ti<sub>5</sub>Si<sub>3</sub> layers formed at the Si<sub>3</sub>N<sub>4</sub> ceramic side in Si<sub>3</sub>N<sub>4</sub>/Kovar brazing with AgCuTi filler. Moreover, Ni can also be found in the brazing seam, which was caused by the dissolution of the GH4169 alloy; thus, Ti<sub>2</sub>Ni can be found in the brazing seam.

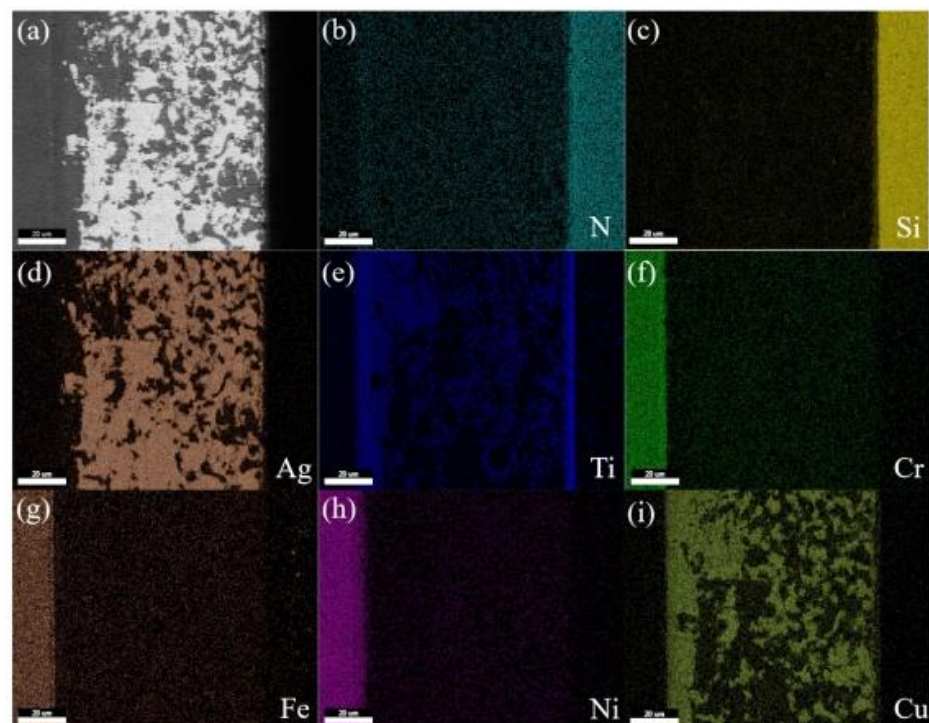


**Figure 7.** GH4169/Si<sub>3</sub>N<sub>4</sub> brazed joint interface (850 °C/15 min): (a) Microstructure; (b–i) main element plane distribution.

According to the above analysis, the formation mechanism of GH4169/Si<sub>3</sub>N<sub>4</sub> joint brazed with AgCuTi filler and Cu foam can be concluded, as shown in Figure 8. Figure 8a,b show the interaction between the substrate and the filler alloy. When heated to the liquid-line temperature of the AgCuTi filler alloy, it began to melt and wet the substrate, the pores of Cu foam are filled with liquid filler. During brazing, Ti diffuses to the Si<sub>3</sub>N<sub>4</sub> ceramics, then reacts with Si<sub>3</sub>N<sub>4</sub> ceramics to form TiN and Ti<sub>5</sub>Si<sub>3</sub> phases, as shown in Figure 8c. The substrate also dissolved into the filler alloy and Ti<sub>2</sub>Ni phase was formed in the reaction layer. The dissolve of Cu form also led to the increase in Cu content in the brazing seam. TiCu compounds were formed at the GH4169 superalloy side.

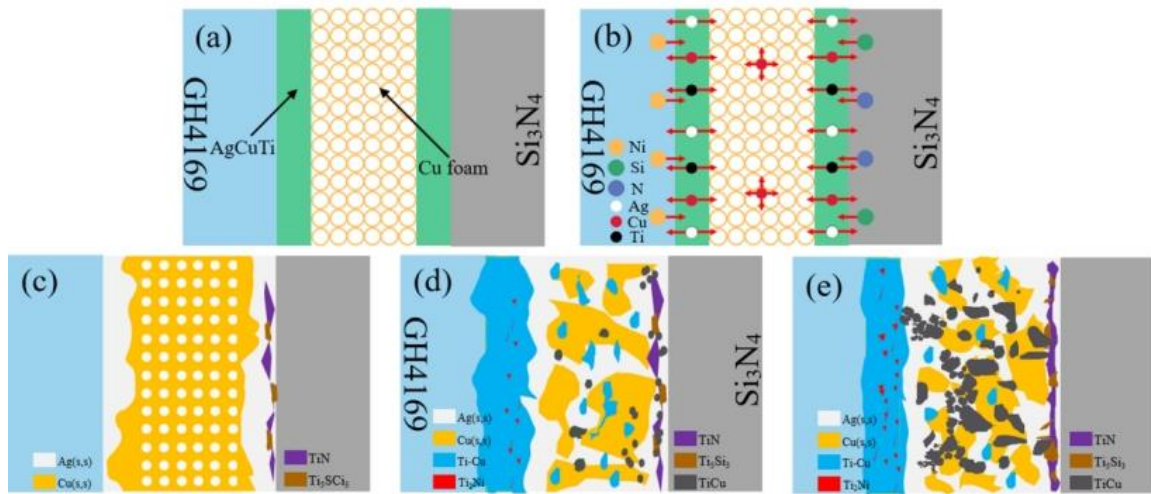


**Figure 8.** Schematic of the GH4169/Si<sub>3</sub>N<sub>4</sub> brazed joint formation mechanism. (a) Brazing interface; (b) filler element begins to diffuse; (c) Cu foam begins dissolution; (d) Cu foam dissolved completely; (e) increase in the TiCu phase.

3.2. Effect of Brazing Temperature on the GH4169/Si<sub>3</sub>N<sub>4</sub> Joint

Figure 9 shows the microstructure of GH4169/Si<sub>3</sub>N<sub>4</sub> joints brazed at different temperatures. No pores, cracks or other defects can be found. The residual Cu(s, s) phase in Cu foam has good plastic deformation ability, which is conducive to relieving the residual stress of the joint [30,31]. Zone II is primarily composed of four different phases: Ag(s, s), Cu(s, s), and Ti-Cu compounds.

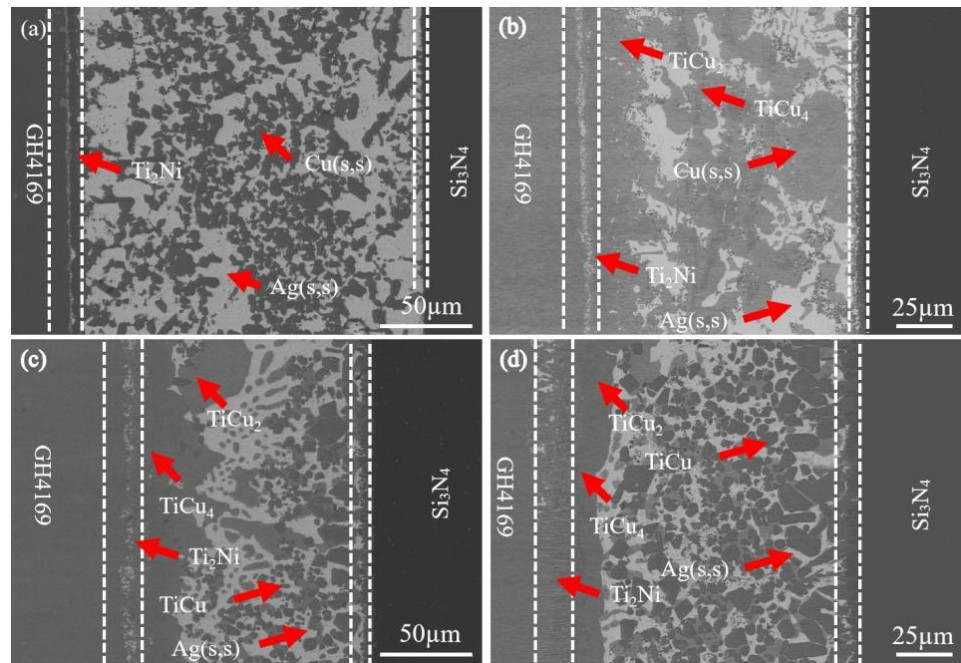


**Figure 9.** Microstructure of the GH4169/Si<sub>3</sub>N<sub>4</sub> joints brazed at different temperatures for 15 min: (a) 820 °C; (b) 850 °C; (c) 880 °C; (d) 910.

The microstructure of the GH4169/Si<sub>3</sub>N<sub>4</sub> joint changed significantly at different brazing temperatures. When brazed at 820°C, the dissolution of AgCuTi filler and Cu foam was limited, the atomic diffusion rate is slow, so more Cu(s,s) can be found in the brazing seam. The reaction between Ti and Si<sub>3</sub>N<sub>4</sub> is also insufficient, no obvious TiN and Ti<sub>5</sub>Si<sub>3</sub> reaction layer was formed at the Si<sub>3</sub>N<sub>4</sub> ceramic side. At GH4169 substrate side, Ti and Cu can react

to form TiCu and TiCu<sub>2</sub>. Due to the dissolve of GH4169 alloy, Ti<sub>2</sub>Ni phase was also formed. At 820 °C, the skeleton structure of Cu foam remains in the brazing seam, and the melt filler fully flows in and a large amount of Ag(s, s) and Cu(s, s) was formed in the brazing seam. The increase in the brazing temperature accelerated the diffusion of elements in the brazing joint, and the thicknesses of zone I and III increased. When the brazing temperature rises to 880 °C, the dissolution of GH4169 superalloy increases, and the diffusion rate of the element increases greatly; thus, more Cu and Ni diffuse to the molten filler alloy, and the volume fraction of Ti<sub>2</sub>Ni and Ti-Cu compounds increases. The collapse of Cu foam also increases the residual stress [32,33] in the brazed joint, which reduces the mechanical properties. When the temperature reaches 910 °C, more Cu is dissolved into the brazing seam. Thus, the volume fraction of the TiCu phase would increase in the brazing seam.

### 3.3. Effect of Brazing Temperature on the Mechanical Properties of the GH4169/Si<sub>3</sub>N<sub>4</sub> Joint

Figure 10 shows the average shear strength of the GH4169/Si<sub>3</sub>N<sub>4</sub> joint brazed at different brazing temperatures. When the brazing temperature increases from 820 °C to 850 °C, the shear strength of the GH4169/Si<sub>3</sub>N<sub>4</sub> joint increases from 164.3 MPa to 196.8 MPa, and then decreases to 122.5 MPa and to 139.7 MPa, respectively, when the brazing temperature further increases to 880 °C and 910 °C. The error of the shear strength is less than 10%. Figure 11 is a comparison diagram of the shear strength of the joint with or without Cu foam brazed at 880 °C. The shear strength of the brazed joint increased from 151.4 MPa to 196.8 MPa. Thus, AgCuTi filler with Cu foam as the intermediate layer is beneficial to alleviate the residual stress, which is caused by the thermal mismatch between ceramic and metal in the brazing process [33,34]. Therefore, the shear strength of the GH4169/Si<sub>3</sub>N<sub>4</sub> joint increased by about 29.9%.

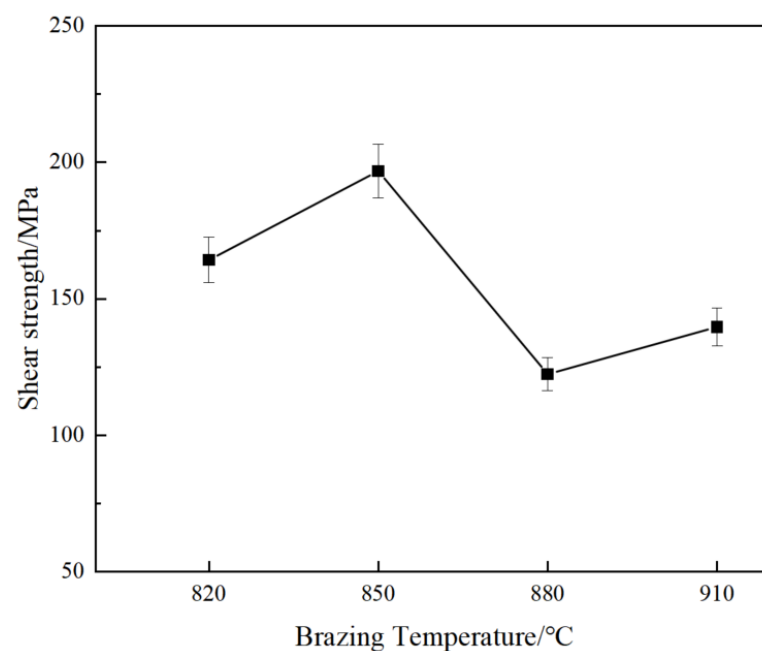


**Figure 10.** Shear strength of the GH4169/Si<sub>3</sub>N<sub>4</sub> joint brazed at different parameters.

When brazed with AgCuTi filler with Cu foam addition, the variation trend of the shear strength can be explained as follows. At lower brazing temperatures, the diffusion rate is low, the reaction between filler metal and substrate is insufficient. Thus, the reaction layer at the Si<sub>3</sub>N<sub>4</sub> side is thin. When the brazing temperature increases, the thickness of the reaction layer increases, and Ag (s, s), Cu (s, s), and Ti-Cu intermetallic compounds are formed in the joint, which is conducive to improving the shear strength of the joint. After further increasing the brazing temperature, the skeleton structure of Cu foam collapses, resulting in the decrease in shear strength. When braze at 910 °C, Cu foam is completely



dissolved, the shear strength of brazing joint increases slightly with the increase in reaction layer thickness on  $\text{Si}_3\text{N}_4$  ceramic side and Ti-Cu intermetallic compounds in joint, but it is still lower than the shear strength at 850 °C [35,36].

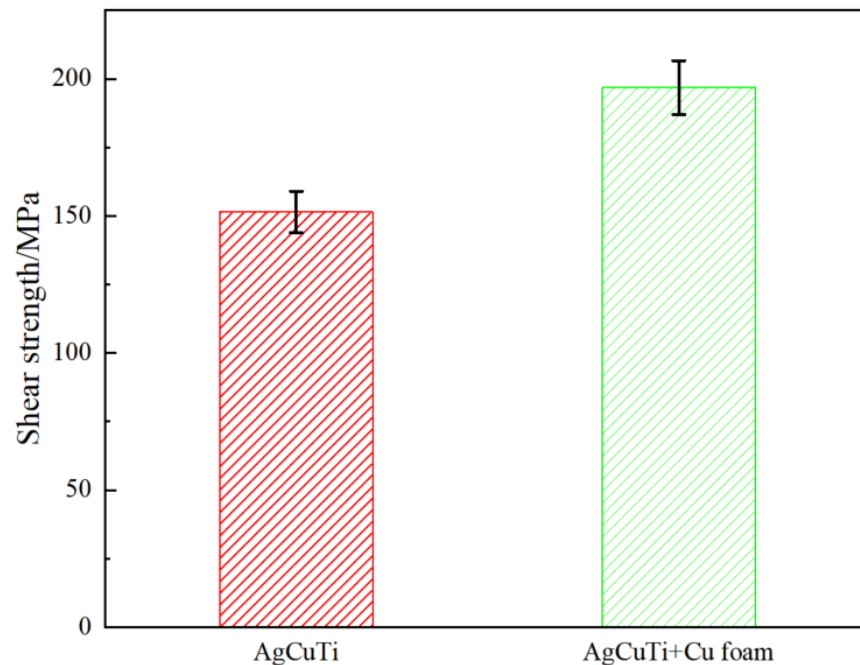


**Figure 11.** Shear strength of brazed joints with and without Cu foam.

In order to further study the relationship between brazing temperature and mechanical properties of the joint, the fracture and fracture path of GH4169/ $\text{Si}_3\text{N}_4$  joint were observed by scanning electron microscope, as shown in Figure 12.

Figure 12a,c,e show that the fracture occurs in  $\text{Si}_3\text{N}_4$  ceramics at 820 °C, 850 °C and 880 °C, indicating that a reliable connection between GH4169 superalloy and  $\text{Si}_3\text{N}_4$  ceramics can be conducted when brazed with AgCuTi filler with Cu foam addition. At 820 °C, the molten filler reacts with  $\text{Si}_3\text{N}_4$  ceramics to form an indistinct reaction layer. The skeleton structure of Cu foam remains in the brazing seam. As a flexible interlayer, Cu foam has good plasticity and plays a role in alleviating the residual stress of the joint. At 850 °C, the thickness of the TiN and  $\text{Ti}_5\text{Si}_3$  reaction layer at the  $\text{Si}_3\text{N}_4$  ceramic side increases, which is conducive to improving the shear strength of the joint. Further increase the brazing temperature, the shear strength began to decrease. At 880 °C, a large number of Ti-Cu intermetallic compounds were formed. The brittle Ti-Cu compounds would result in crack initiation and propagation. Dimples can be found in the fracture shown in Figure 12f, indicating that the increasing of ductility of the brazing joint. At higher temperature, the shear strength of brazing joint increases slightly with the increase in reaction layer thickness on  $\text{Si}_3\text{N}_4$  ceramic side and Ti-Cu intermetallic compounds in the joints.

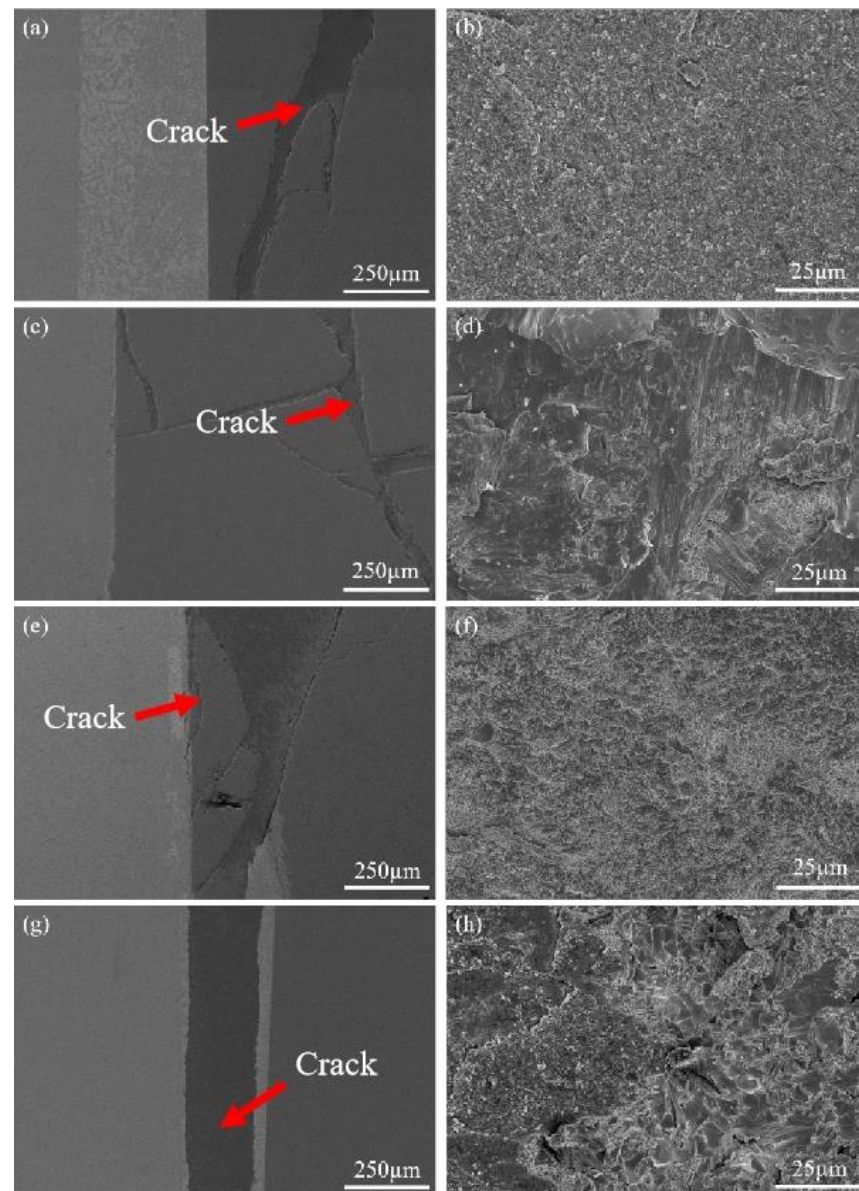


**Figure 12.** Fracture path and morphology of the GH4169/Si<sub>3</sub>N<sub>4</sub> joints at different temperatures: (a,b) 820 °C; (c,d) 850 °C; (e,f) 880 °C; and (g,h) 910 °C.

#### 4. Conclusions

GH4169 superalloy and Si<sub>3</sub>N<sub>4</sub> ceramics were brazed by AgCuTi filler with Cu foam addition. The effects of different brazing temperatures on the microstructure and mechanical properties of GH4169/Si<sub>3</sub>N<sub>4</sub> joints were studied. The conclusions are as follows:

- (1) The GH4169/Si<sub>3</sub>N<sub>4</sub> joints can be divided into three zones. The microstructure of the joint is GH4169 superalloy/TiCu+Ti<sub>2</sub>Ni+TiCu<sub>2</sub>+Ag (s,s)+TiCu<sub>4</sub>+Cu (s,s)+TiN+Ti<sub>5</sub>Si<sub>3</sub>/Si<sub>3</sub>N<sub>4</sub> ceramics.
- (2) During brazing, the Ti elements in the AgCuTi filler would react with the substrate. The aggregate on the side of the GH4169 superalloy to form Ti-Cu intermetallic compounds and a continuous reaction layer of TiN and Ti<sub>5</sub>Si<sub>3</sub> were formed. With the gradual dissolution of Cu foam, and the content of Cu (s, s) in the joint is reduced. The increase in Ag (s, s), Cu (s, s) and reaction layer thickness in the joint is conducive to the improvement of the mechanical properties of the joint.
- (3) At 850 °C, the shear strength of the joint reaches a maximum of 196.85 MPa. With the increase in brazing temperature, the skeleton of Cu foam disappeared, and the

volume fraction of Ti-Cu intermetallic compounds increased, which is harmful to the mechanical properties.

**Author Contributions:** Conceptualization, X.Y. and Y.X.; methodology, Y.X.; software, X.Y.; validation, X.Y., Y.X. and Z.Z.; formal analysis, X.Y. and Y.X.; investigation, Z.Z. and J.G.; resources, Z.Z. and J.T.; data curation, X.Y. and Y.X.; writing—original draft preparation, X.Y. and Y.X.; writing—review and editing, X.Y. and Y.X.; visualization, J.X. and S.W.; supervision, J.G. and Y.C.; project administration, J.T. and S.W.; funding acquisition, X.Y. and Y.C. All authors have read and agreed to the published version of the manuscript.

**Funding:** This research was funded by the National Natural Science Foundation of China, Grant Nos. 52071165 and 51771083) and Jinhua non-profit technological application research project (No.: 2022-4-012).

**Institutional Review Board Statement:** Not applicable.

**Informed Consent Statement:** Not applicable.

**Data Availability Statement:** Not applicable.

**Conflicts of Interest:** The authors declare no conflict of interest.

## References

1. Fei, S.O.; Ryotaro, N.; Hirobumi, T.; Eiichi, S. Strength optimization of two-step-bonded Ti-6Al-4V/Si<sub>3</sub>N<sub>4</sub> joint with Nb interlayer via transient-liquid-phase bonding and active-metal brazing. *J. Eur. Ceram. Soc.* **2022**, *42*, 2707–2717.
2. Li, M.; Shi, K.Q.; Zhu, D.D.; Dong, D.; Liu, L.; Wang, X.H. Microstructure and mechanical properties of Si<sub>3</sub>N<sub>4</sub> ceramic and (TiB+Y<sub>2</sub>O<sub>3</sub>)/Ti matrix composite joints brazed with AgCu/Cu foam/AgCu multilayered filler. *J. Manuf. Process.* **2021**, *66*, 220–227. [[CrossRef](#)]
3. Wei, C.C.; Zhang, Z.Y.; Ma, X.F.; Liu, L.Y. Mechanical and ablation properties of laminated ZrB<sub>2</sub>-SiC ceramics with Si<sub>3</sub>N<sub>4</sub> whisker interface. *Corros. Sci.* **2022**, *197*, 110051. [[CrossRef](#)]
4. Zhang, Z.Q.; Shi, K.Q.; Huang, X.C.; Shi, Y.Y. Development of a probabilistic algorithm of surface residual materials on Si<sub>3</sub>N<sub>4</sub> ceramics under longitudinal torsional ultrasonic grinding. *Ceram. Int.* **2022**, *48*, 12028–12037. [[CrossRef](#)]
5. Zhang, Z.; Li, J.N.; Sun, X.G.; Ma, F.K. Microstructure performance enhancement of Si<sub>3</sub>N<sub>4</sub> reinforced laser clad KF110 base composite coatings. *Int. J. Appl. Ceram. Technol.* **2022**, *19*, 409–414. [[CrossRef](#)]
6. Srivastava, A.K.; Dwivedi, S.; Saxena, A.; Kumar, D. Tribological Characteristics of Al359/Si<sub>3</sub>N<sub>4</sub>/Eggshell Surface Composite Produced by Friction Stir Processing. *Coatings* **2022**, *12*, 1362. [[CrossRef](#)]
7. Kour, P.; Pradhan, S.K.; Kumar, A.; Kar, M. Machining by Advanced Ceramics Tools: Challenges and Opportunities. In *Advances in Sustainable Machining and Manufacturing Processes*; CRC Press: Boca Raton, FL, USA, 2022; Volume 14, pp. 17–30.
8. Gao, W.; Wang, L.Q.; Jin, Y.H.; Yao, Y.H. Effect of Si<sub>3</sub>N<sub>4</sub>/TaC Particles on the Structure and Properties of Microarc Oxidation Coatings on TC4 Alloy. *Coatings* **2022**, *12*, 1247. [[CrossRef](#)]
9. Salmi, M. Additive manufacturing processes in medical applications. *Materials* **2021**, *14*, 191. [[CrossRef](#)]
10. Zhang, J.Y.; Yan, M.W.; Sun, G.C.; Liu, L.Q. An environment-friendly Fe<sub>3</sub>O<sub>4</sub>@CFAS porous ceramic: Adsorption of Cu(II) ions and process optimisation using response surface methodology. *Ceram. Int.* **2021**, *476*, 8256–8264. [[CrossRef](#)]
11. Dubois, P.K.; Landry, C.; Thibault, D.; Plante, J.S. Benefits and Challenges of the Inside-Out Ceramic Turbine: An Experimental Assessment. *J. Propuls. Power* **2022**, *38*, 221–228. [[CrossRef](#)]
12. Zhao, Y.X.; Bian, H.; Fu, W.; Hu, Y. Laser-induced metallization of porous Si<sub>3</sub>N<sub>4</sub> ceramic and its brazing to TiAl alloy. *J. Am. Ceram. Soc.* **2019**, *102*, 32–36. [[CrossRef](#)]
13. Guo, W.; Zhang, H.Q.; Ma, K.T.; Zhu, Y. Reactive brazing of silicon nitride to Invar alloy using Ni foam and AgCuTi intermediate layers. *Ceram. Int.* **2019**, *45*, 13979–13987. [[CrossRef](#)]
14. Ahn, B. Recent advances in brazing fillers for joining of dissimilar materials. *Metals* **2021**, *11*, 1037. [[CrossRef](#)]
15. Zheng, J.J.; Guo, Y.; Liu, X.; Zhang, Z.T. Introduction on Research and Application of Nickel Base Superalloy GH4169. *IOP Conf. Ser. Earth Environ. Sci.* **2021**, *651*, 022081. [[CrossRef](#)]
16. Xiao, G.J.; Xing, J.Z.; Zhang, Y.D. Surface roughness prediction model of GH4169 superalloy abrasive belt grinding based on multilayer perceptron(MLP). *Procedia Manuf.* **2021**, *54*, 269–273. [[CrossRef](#)]
17. Chen, W.; Zhang, P.; Xie, J.; Liu, Y. Metallurgical Analysis of different processing technologies on tensile behavior of GH4169 superalloy. *IOP Conf. Ser. Earth Environ. Sci.* **2021**, *772*, 012066. [[CrossRef](#)]
18. Seleznev, A.; Pinargote, N.W.S.; Smirnov, A. Ceramic Cutting Materials and Tools Suitable for Machining High-Temperature Nickel-Based Alloys: A Review. *Metals* **2021**, *11*, 1385. [[CrossRef](#)]
19. Guo, W.; Li, K.; Zhang, H.Q.; Zhu, Y. Low residual stress C/C composite-titanium alloy joints brazed by foam interlayer. *Ceram. Int.* **2022**, *48*, 5260–5266. [[CrossRef](#)]

20. Wang, G.; Cai, Y.J.; Wang, W.; Gui, K.X.; Zhu, D.D.; Tan, C.W.; Cao, W. Brazing ZrB<sub>2</sub>-SiC ceramics to Inconel 600 alloy without and with Cu foam. *J. Manuf. Process.* **2019**, *41*, 29–35. [[CrossRef](#)]
21. Wang, X.Y.; Li, C.; Si, X.Q.; Qi, J.L. Brazing ZTA ceramic to TC4 alloy using the Cu foam as interlayer. *Vacuum* **2018**, *155*, 7–15. [[CrossRef](#)]
22. Liu, G.P.; Li, Y.L.; Long, W.F.; Hu, X.W. Wetting kinetics and spreading phenomena of the precursor film and bulk liquid in the AgCuTi/TC4 system. *J. Alloys Compd.* **2019**, *802*, 345–354. [[CrossRef](#)]
23. Zhao, Y.X.; Song, X.G.; Tan, C.W.; Hu, S.P. Microstructural evolution of Si<sub>3</sub>N<sub>4</sub>/Ti6Al4V joints brazed with nano-Si<sub>3</sub>N<sub>4</sub> reinforced AgCuTi composite filler. *Vacuum* **2017**, *142*, 58–65. [[CrossRef](#)]
24. Gui, X.Y.; Zhang, M.F.; Zhang, X.T.; Guo, Q.H. Theoretical Investigations on Interfacial Behavior of Ag–Cu–Ti/Si<sub>3</sub>N<sub>4</sub> Wetting System. *J. Nanoelectron. Optoelectron.* **2021**, *16*, 1780–1790. [[CrossRef](#)]
25. Dong, D.; Zhu, D.D.; Wang, Y.; Wang, G.; Wu, P. Microstructure and shear strength of brazing TiAl/Si<sub>3</sub>N<sub>4</sub> joints with Ag-Cu binary alloy as filler metal. *Metals* **2018**, *8*, 896. [[CrossRef](#)]
26. Zhang, Y.; Guo, X.M.; Guo, W.; Zhang, H.Q. Effect of Cu foam on the microstructure and strength of the SiC<sub>f</sub>/SiC-GH536 brazed joint. *Ceram. Int.* **2022**, *48*, 12945–12953. [[CrossRef](#)]
27. Guo, X.J.; Si, X.Q.; Li, C.; Zhao, S.H.; Liu, Y.X. Active brazing of C/C composites and single crystal Ni-based superalloy: Interfacial microstructure and formation mechanism. *J. Alloys Compd.* **2021**, *886*, 161183. [[CrossRef](#)]
28. Xin, C.L.; Yan, J.Z.; Wang, Q.Y.; Feng, W. The microstructural evolution and formation mechanism in Si<sub>3</sub>N<sub>4</sub>/AgCuTi/Kovar braze joints. *J. Alloys Compd.* **2020**, *820*, 153189. [[CrossRef](#)]
29. Wang, Y.; Jin, C.K.; Yang, Z.W.; Wang, D.P. Effects of Cu interlayers on the microstructure and mechanical properties of Al<sub>2</sub>O<sub>3</sub>/AgCuTi/Kovar brazed joints. *Int. J. Appl. Ceram. Technol.* **2019**, *16*, 896–906. [[CrossRef](#)]
30. Wang, G.; Cai, Y.; Xu, Q.; Zhou, C. Microstructural and mechanical properties of inconel 600/ZrB<sub>2</sub>-SiC joints brazed with AgCu/Cu-foam/AgCu/Ti multi-layered composite filler. *J. Mater. Res. Technol.* **2020**, *9*, 3430–3437. [[CrossRef](#)]
31. Wang, Z.; Wang, G.; Li, M.; Lin, J.M. Three-dimensional graphene-reinforced Cu foam interlayer for brazing C/C composites and Nb. *J. Carbon.* **2017**, *118*, 723–730. [[CrossRef](#)]
32. Li, M.N.; Wang, Z.Y.; Ba, J.; Ma, Q. In-Situ synthesized TiC nano-flakes reinforced C/C composite-Nb brazed joint. *J. Eur. Ceram. Soc.* **2018**, *38*, 1059–1068.
33. Guo, W.; Xue, J.L.; Zhang, H.Q.; Cui, H. The role of foam on microstructure and strength of the brazed C/C composites/Ti6Al4V alloy joint. *Vacuum* **2020**, *179*, 109543. [[CrossRef](#)]
34. Zahri, N.A.M.; Yusof, F.; Miyashita, Y.; Ariga, T. Brazing of porous copper foam/copper with amorphous Cu-9.7Sn-5.7Ni-7.0P (wt%) filler metal: Interfacial microstructure and diffusion behavior. *Weld. World* **2020**, *64*, 209–217. [[CrossRef](#)]
35. Ahmed, S.A.; Hasanabadi, M.F.; Kumar, A.V. Joining of ceramic to metal by friction welding process: A review. *Proc. Inst. Mech. Eng. Part L-J. Mater.-Des. Appl.* **2021**, *235*, 1723–1736. [[CrossRef](#)]
36. Wang, Y.; Yang, Z.W.; Zhang, L.X.; Feng, J.C. Microstructure and Mechanical Properties of Invar Alloy and Si<sub>3</sub>N<sub>4</sub> Ceramic Brazed Joints. *Rare Met. Mater. Eng.* **2015**, *44*, 339–343.